Chemistry–A European Journal
Research Article
doi.org/10.1002/chem.202301752
Chemistry Europe
European Chemical Societies Publishing
www.chemeurj.org

Hot Paper

Special Collection

A General Pathway towards NHC·GaH$_2$(OTf) Adducts – The Key for the Synthesis of NHC-Stabilized Cationic 13/15 Chain Compounds of Gallium

Robert Szlosek,[a] Michael Seidl,[a] Gábor Balázs,[a] and Manfred Scheer*[a]

A general pathway towards NHC (NHC = N-heterocyclic carbene)-stabilized galliummonotriflates NHC·GaH$_2$(OTf) (NHC = IDipp, **1 a**; IPr$_2$Me$_2$, **1 b**; IMes, **1 c**; IDipp = 1,3-bis(2,6-diisopropylphenyl)-imidazolin-2-ylidene, IPr$_2$Me$_2$ = 1,3-bis-(diisopropyl)-4,5-dimethyl-imidazolin-2-ylidene, IMes = 1,3-bis(2,4,6-trimethylphenyl)-imidazolin-2-ylidene) is reported. Quantum chemical calculations give detailed insight into the underlying reaction pathway. The obtained NHC·GaH$_2$(OTf) compounds were employed in reactions with donor-stabilized pnictogenylboranes to synthesize the elusive cationic parent 13/15/13 chain compounds [IDipp·GaH$_2$ER$_2$E′H$_2$·D][OTf] (**3 a**: D = IDipp, E = P, E′ = B, R = H; **3 b**: D = NMe$_3$, E = P, E′ = B, R = H, **3 c**: D = NMe$_3$, E = P, E′ = B, R = Ph, **3 d**: D = IDipp, E = P, E′ = Ga, R = H). Supporting computational studies highlight the electronic features of the products.

Introduction

Semiconductor materials such as GaAs represent the backbone of almost all modern digital devices. In industry, thin layers of, for example, GaAs are obtained by metal–organic chemical vapor deposition (MOCVD) from GaMe$_3$ and AsH$_3$.[1] With the rapidly increasing demand for smaller and more powerful electronics, the research for suitable 13/15 compounds as useful precursor compounds has expanded. The first milestones in this field were, however, already set a long time ago, starting with compounds such as H$_3$N·BF$_3$, borazine and Me$_3$N·BH$_3$.[2] Compared to their organic counterparts, the 13/15 compounds differ in terms of their reactivity and physical properties due to polarized bonding. The chemistry of 13/15 compounds was especially pushed by the concept of single-source precursors in the late 20th century, where a group 13 and a group 15 element are fixed in a single compound that can then be used for MOCVD processes.[3] Of special interest are the parent hydrogen-bearing compounds that are isoelectronic to their organic counterparts (i.e., H$_2$E-MH$_2$→H$_2$C=CH$_2$, HE=MH→HC≡CH; E = triel, M = pnictogen) and are lighter in molecular weight and thus, more volatile than their alkyl-substituted versions. Besides possessing a well-defined stoichiometry for controlled deposition, the atomic diversity of 13/15 substrates is beneficial for achieving unusual materials. Besides applications for the semiconductor industry, 13/15 compounds are also considered as candidates for lightweight hydrogen storage materials.[4]

Typical 13/15 monomers are prone to undergoing spontaneous head-to-tail oligo- or polymerization and thus require additional stabilization (Figure 1).[5] The easiest way to achieve this, is by a donor system such as tertiary amines, β-diketiminates (Nacnac) or *N*-heterocyclic carbenes (NHC, type **A**). Especially with NHCs and Nacnac donor systems, a huge variety of 13/15 compounds was enabled ranging from the parent phosphanyl, arsanyl and stibanyl gallanes to phosphanyl phosphagallenes and many other spectacular results.[6] Also, simultaneous stabilization by an acceptor and a donor attached to the monomer has been used in the past for the stabilization of parent phosphanylalanes (type **B**).[7] Although plausible, stabilization by a single acceptor only (type **C**) has not been realized experimentally so far.

Furthermore, bulky organic residues play a crucial role in the stabilization of the said monomers and other low-valent group 13 species, especially with emphasis on their versatile use as Frustrated Lewis Pairs (FLPs) in synthesis and catalysis.[8]

In the past, our group showed that trimethylamine-stabilized pnictogenylboranes can be functionalized with neutral,[9,10,11] anionic[12] or cationic fragments,[9,10,13–15] leading to elongated chain-like 13/15 monomers (Figure 2). In the latter case, three- or even five-membered chain compounds could be obtained by reaction of NMe$_3$·BH$_2$EH$_2$ with BH$_2$I·NMe$_3$ or 0.5 BH$_2$I·SMe$_2$, respectively (E = P, As).[14,15] Besides these catenation reactions, controlled oligo/polymerization,[10,16] coordination[10,17] and oxidation capabilities of Lewis base-stabilized pnictogenylboranes could also be demonstrated.[9,18] In all of these reactions, boron was used as group 13 element because of the high stability of the resulting products.

However, analogous parent chain compounds with the heavier group 13 homologues are unknown so far. Investiga-

[a] R. Szlosek, Dr. M. Seidl, Dr. G. Balázs, Prof. Dr. M. Scheer
Institut für Anorganische Chemie
Universität Regensburg
93053 Regensburg (Germany)
E-mail: manfred.scheer@ur.de
Homepage: http://www.uni-regensburg.de/chemie-pharmazie/anorganische-chemie-scheer

Supporting information for this article is available on the WWW under https://doi.org/10.1002/chem.202301752

Part of a Special Collection on the p-block elements.

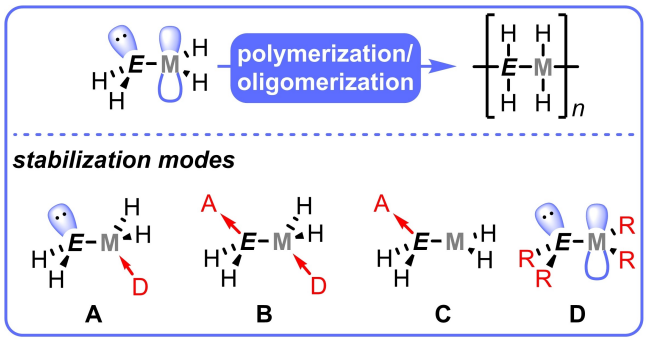

Figure 1. Different stabilization modes of 13/15 monomeric compounds (E = group 15 element, M = group 13 element): A) stabilization by only a single donor, B) stabilization by simultaneous donor and acceptor interaction, C) stabilization by acceptor only, D) stabilization by bulky organic residues.

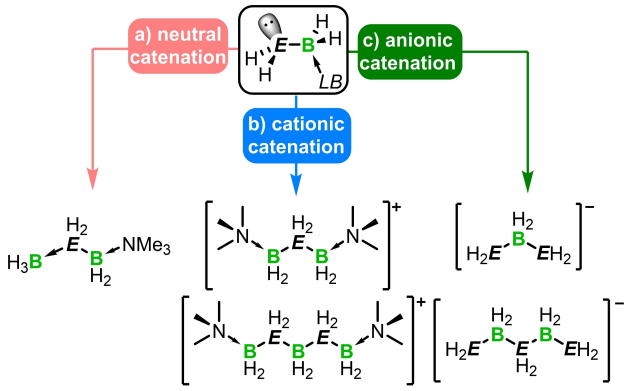

Figure 2. Overview of *catena* extensions of Lewis base-stabilized parent pnictogenylborane monomers (E = P, As; LB = Lewis base). Description of depicted pathways: a) reaction with neutral group 13 sources such as $BH_3 \cdot SMe_2$, b) reaction with suitable $[BH_2]^+$ synthons such as $Me_3N \cdot BH_2I$ or $Me_2S \cdot BH_2I$, c) reaction with group 15 $[EH_2]^-$ sources such as $NaPH_2$ or $KAsH_2$.

tions on these compounds are hampered by the intrinsically low bond energies between the heavy group 13 elements and phosphorus or arsenic, often resulting in the extreme sensitivity of such products towards air and thermal decomposition already at room temperature.[19–21] Furthermore, the needed monomers themselves are difficult to generate in larger quantities, which are necessary for in-depth studies.[19,20] Thus, the question arises as to whether especially charged 13/15 chain compounds including group 13 elements heavier than boron are accessible at all, despite the low tendency to form stable bonds, and which donors would be suitable to keep the core motifs intact. Herein, the preparation of novel NHC-stabilized galliummonotriflates is reported, which were used for the synthesis of unprecedented cationic 13/15/13 chains with $\{GaH_2\}$ links, stabilized by two separate donor systems.

Results and Discussion

First, the reactivity of NHC-stabilized phosphanylgallane IDipp·GaH_2PH_2 with suitable group 13 electrophiles which could enable cationic catenation was investigated. Therefore, reactions with $BH_2I \cdot NMe_3$ were attempted (Scheme 1). However, no reaction was observed, since the nucleophilicity of IDipp·GaH_2PH_2 is too low to substitute iodide from $BH_2I \cdot NMe_3$. Even if iodide was replaced by the superior leaving group triflate, no reaction took place. Then, reactions of $BH_2Cl \cdot NMe_3$ in the presence of halide abstractors such as $AlCl_3$ and Tl[TEF] (TEF = $[Al\{OC(CF_3)_3\}]^-$) were attempted,[22] which, unfortunately, led to the decomposition of the starting material, presumably via cleavage of the Ga–P bond. The introduction of alkyl groups at the phosphorus atom did not provide steps forward towards the desired reactivity.

A different approach to the targeted products could be realized by reversing the reaction principle and combining donor-stabilized phosphanylboranes $D \cdot BH_2PH_2$ with a $[NHC \cdot GaH_2]^+$ synthon such as IDipp·GaH_2I described by Radius et al.[23] According to preliminary NMR data, these reactions showed full conversion of the starting material (see Supporting Information). However, it was not possible to grow single crystals for X-ray structure determination for an unambiguous proof of connectivity. Thus, as an alternative, we targeted the introduction of a different leaving group such as triflate (OTf = $[SO_3CF_3]^-$) at the Ga atom. Interestingly, such starting materials have not been described in literature. The addition of Me(OTf) to a solution of NHC·GaH_3 (NHC = IDipp (1,3-Bis-(2,6-diisopropylphenyl)-imidazolin-2-ylidene, **1 a**), IMes (1,3-Bis-(2,4,6-trimethylphenyl)-imidazolin-2-ylidene, **1 b**), IPr_2Me_2 (1,3-Bis-(diisopropyl)-4,5-dimethylimidazolin-2-ylidene, **1 c**) in toluene results in a visible extrusion of methane and the precipitation of the unprecedented galliummonotriflates NHC·GaH_2(OTf) (Scheme 2a). After work-up, the compounds are obtained as air-sensitive colourless solids in isolated yields between 77–88% that can be stored for months under an inert atmosphere at −30 °C.

Alternatively, by reacting IDipp·GaH_2Cl with Ag(OTf) (Scheme 2b), similar products can also be synthesized by salt metathesis, which gives somewhat lowered yields and needs an additional filtration step. The ^1H NMR spectra of **1 a–c** show characteristic, broadened singlets for the GaH_2 unit at 4.88 ppm (**1 a**, C_6D_6, 2 H), 4.22 ppm (**1 b**, CD_2Cl_2, 2 H), and 5.62 ppm (**1 c**, C_6D_6, 2 H), besides the characteristic signals of the corresponding NHC moieties. The $^{19}F\{^1H\}$ NMR spectra of all three compounds show a singlet between −77.3 and −77.6 ppm for bound $[OTf]^-$ moieties, which is slightly shifted downfield compared to the unbound $[OTf]^-$ anion (−79 ppm, cf. Supporting Information). The mass spectra reveal peaks of

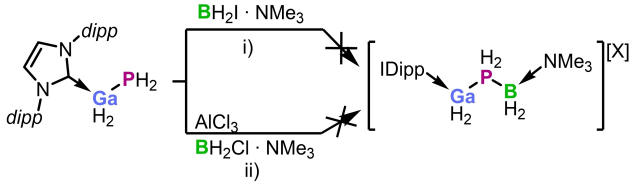

Scheme 1. Attempted cationic catenations of IDipp·GaH_2PH_2 with $BH_2I \cdot NMe_3$ and $BH_2Cl \cdot NMe_3/AlCl_3$. Reaction conditions: i) Et_2O, −80 °C→r.t., 16 h; ii) CH_2Cl_2, −80 °C→r.t., 2 h.

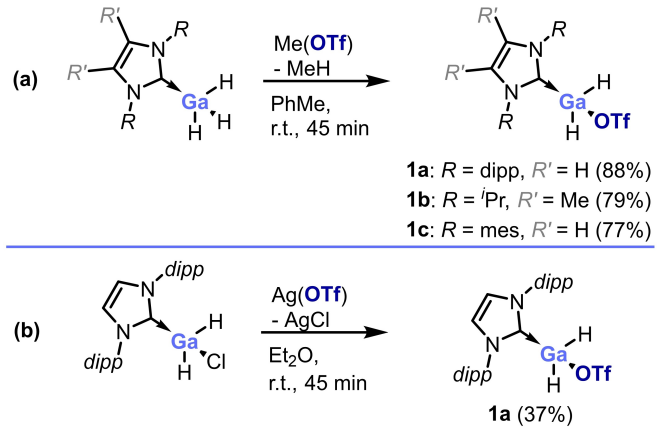

Scheme 2. Synthesis of NHC-stabilized galliummonotriflates by elimination of methane (a) or salt metathesis with Ag(OTf) (b). Isolated yields are given in parentheses.

$[IDipp{\cdot}GaH_2]^+$ at $m/z = 459.25$ (**1 a**, LIFDI-MS), $[IPr_2Me_2{\cdot}GaH_2]^+$ at $m/z = 253.11$ (**1 b**, ESI-MS), and $[IMes{\cdot}GaH_2]^+$ at $m/z = 375.31$ (**1 c**, ESI-MS). Single crystals of **1 a** were grown by slow evaporation of a concentrated solution in benzene and of **1 b** by cooling a saturated solution in toluene to −28 °C overnight. Unfortunately, all attempts at crystallizing **1 c** have failed so far. **1 c** can be readily isolated as a microcrystalline powder though.

1 a crystallizes in the acentric orthorhombic space group $P2_12_12_1$ as clear colourless block-shaped crystals (Figure 3; Flack parameter: −0.016(8)). The asymmetric unit shows one formula unit of IDipp·GaH$_2$(OTf). The triflate group is arranged almost perpendicular to the {CGaH$_2$} part with a $C_{carbene}$–Ga–O angle of 99.27(9)°, indicative of weak bonding towards the gallium atom with a long Ga–OTf distance of 1.991(2) Å. This distance is also well above the sum of covalent radii of a Ga–O single bond (1.87 Å),[24] underlining this weak interaction. Overall, the structure is more resembling of a $[IDipp{\cdot}GaH_2]^+$ ion with a loose interaction of the triflate ion.

1 b crystallizes in the orthorhombic space group *Pbca* as clear colourless prism-shaped crystals. The asymmetric unit shows one formula unit of $IPr_2Me_2{\cdot}GaH_2(OTf)$. When grown, the crystal structure reveals a one-dimensional polymeric network with μ_2-bridging triflates as a zigzag chain (Figure 4). The NHC units are oriented perpendicular to each other around the main $\{GaOTf\}_\infty$ strand. The O–Ga distance is extremely long and lies between 2.3777(15)–2.2533(15) Å but still well below the sum of the van der Waals radii (3.39 Å). The O–Ga–O angle of 174.64(5)° is close to 180° and together with a $C_{carbene}$–Ga–O angle of 86.10(7)–88.54(7)° highlights the slightly distorted trigonal bipyramidal structure. Overall, all this nicely illustrates the influence of the sterics of the NHC on the molecular structure of these adducts, as the larger NHCs in, for example, **1 a** prevent the formation of polymeric structures.

Interestingly, several similar reactions are described in the literature. Rivard and co-workers reacted IMes·GaH$_3$ with Me(OTf) in CH_2Cl_2 over the course of 16 h and observed exclusively di-triflation leading to IMes·GaH(OTf)$_2$.[25] On the other hand, Radius and coworkers could selectively synthesize NHC·GaH$_2$I by the analogous reaction of NHC·GaH$_3$ with a large excess of MeI in toluene.[23] To compare our results with the results achieved by the Rivard and Radius groups, experimental and theoretical investigations were performed. As MeI displays a slightly lower reactivity than Me(OTf) and thus slower reaction progress, the sequential iodination of IDipp·GaH$_3$ with MeI was chosen as a model system as this allowed for easier reaction monitoring. First, the influence of the solvent used was tested. The reaction of IDipp·GaH$_3$ in the presence of an excess amount of MeI in CH_2Cl_2 or toluene (30-45 min) at room temperature in both cases yields exclusively the mono-iodinated product according to ^{1}H NMR spectroscopy, upon which the influence of the solvent regarding the product formation could be excluded. When the stirring time is increased to 16 h however, full conversion towards di-iodinated IDipp·GaHI$_2$ is observed by ^{1}H NMR spectroscopy (Eq. (1), Fig-

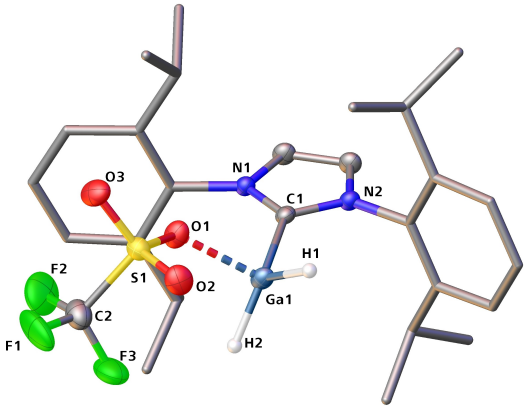

Figure 3. Molecular structure of **1 a** in the solid state. Anisotropic displacement ellipsoids are shown at 50% probability level. Hydrogen atoms bound to carbon are omitted for clarity. Dipp groups are displayed as a stick model for improved clarity. Selected bond lengths [Å] and angles [°]: N1–C1 1.350(3), N2–C1 1.347(3), C1–Ga1 2.039(3), Ga1–H1 1.51(4), Ga–H2 1.49(4), Ga1–O1 1.991(2), O1–S1 1.4781(19), S1–O2 1.427(2), S1–O3 1.427(2), S1–C2 1.822(3), C2–F1 1.328(4), C2–F2 1.318(4), C2–F3 1.327(4), N1–C1–Ga1 130.94(19), N2–C1–Ga1 123.62(18), C1–Ga1–O1 99.27(9), C1–Ga1–H1 113.5(14), C1–Ga–H2 113.7(14), H1–Ga1–H2 123(2), Ga1–O1–S1 127.35(12).

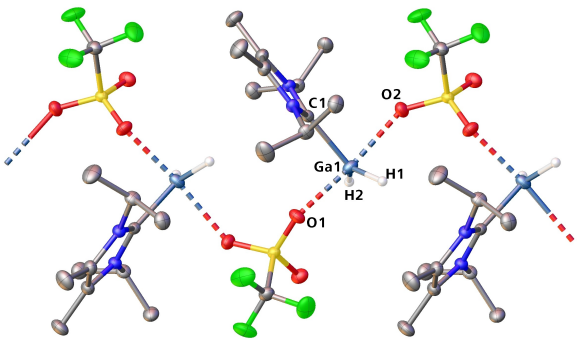

Figure 4. 1D polymeric structure of **1 b** in the solid state. Anisotropic displacement ellipsoids are shown at 50% probability level. Hydrogen atoms bound to carbon are omitted for clarity. Selected bond lengths [Å] and angles [°]: C1–Ga1 2.0281(19), Ga1–H1 1.46(2), Ga1–H2 1.46(3), Ga1–O2 2.3777(15), Ga1–O1 2.2533(15), C1–Ga1–O1 88.54(7), C1–Ga1–O2 86.10(7), H1–Ga1–H2 126.8(13), C1–Ga1–H1 117.0(9), C1–Ga1–H2 115.8(10), O1–Ga1–O2 174.64(5).

ure 5). This result indicates that the first reaction step happens almost instantaneously, which then deactivates the hydrides bound to the gallium atom and hence drastically slows down the reaction rate for the second reaction with MeI. It was also tested, if full conversion to IDipp·GaI_3 is possible by reacting IDipp·GaH_3 with an excess amount of MeI in boiling toluene overnight. According to ^{1}H NMR spectroscopy, no gallium hydride peak is found anymore (see Supporting Information), which indicates full conversion of the starting material as well as the intermediates. However, the spectrum clearly shows a product mixture of several species, which might be the result of ongoing side reactions.

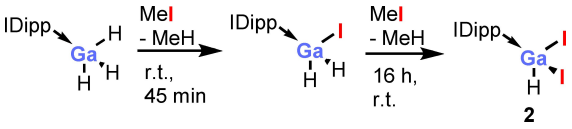

To further probe our assumptions, we performed quantum chemical calculations at the robust DLPNO-CCSD(T)/def2-QZVP//B3LYP-D4/def2-TZVP[26,27,28] level of theory on the model reaction of IPr_2Me_2·GaH_3 in three subsequent iodination steps (see Supporting Information). The calculated reaction pathway shows that all three iodination steps are exergonic and therefore show favourable thermodynamics. Most importantly though, the second transition state lies +3.42 kcal mol^{-1} higher in energy than the first.

According to the transition state theory by Eyring and Polanyi,[29] the first iodination is faster compared to the second by $k_1 = 325 \times k_2$ at $T = 298$ K, which agrees with the observed reactivity. For the still bulkier IDipp or IMes, an even more pronounced difference in reaction rates could be expected.

With the novel NHC-stabilized galliummonotriflates at hand, it was then possible to address the question as to whether reactions of pnictogenylboranes lead to new cationic 13/15 chain compounds containing gallium. Therefore, IDipp·BH_2PH_2 was reacted with **1a** by stirring for 30 min at room temperature in *o*-difluorobenzene (Eq. (2)).[32] NMR spectroscopic monitoring revealed full conversion of the starting material after this time (see Supporting Information). By layering the solution with *n*-hexane at −30 °C, large single crystals of the unprecedented 13/15 cationic chain compound [IDipp·$GaH_2PH_2BH_2$·IDipp][OTf] (**3a**) were obtained (Figure 6). Characteristic NMR spectroscopic data are summarized in Table 1. Note that all signals in the ^{31}P and ^{11}B NMR spectra appear strongly broadened due to quadrupolar relaxation induced by the boron and gallium nuclei ($\omega_{1/2} > 100$ Hz). **3a** also shows a characteristic doublet in the ^{1}H NMR spectrum for the {GaH_2} unit with a coupling constant of $^2J_{HP} = 38$ Hz. The molecular ion peak for **3a** is detected in the ESI-MS spectrum at $m/z = 893.53$.

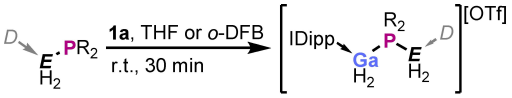

3a: *D* = IDipp, ***E*** = **B**, R = H, 46%
3b: *D* = NMe_3, ***E*** = **B**, R = H, 42%
3c: *D* = NMe_3, ***E*** = **B**, R = Ph, 72%
3d: *D* = IDipp, ***E*** = **Ga**, R = H, 50%

3a crystallizes in the monoclinic space group $P2_1/c$ as clear colourless blocks (Figure 6, top left), which are highly air- and temperature-sensitive. The asymmetric unit shows one molecule of **3a**, which is disordered at all chain atom positions (see Supporting Information). The core chain motif shows Ga–P and B–P bond distances of the range of classic single bonds with 2.379(7) Å (Ga–P, cf. IDipp·GaH_2PH_2: 2.3373(6) Å) and 1.949(10) Å (P–B, cf. Me_3N·BH_2PH_2: 1.976(2) Å). The Ga–P–B angle of 103.8(3)° is considerably smaller compared to the B–P–B angle within [Me_3N·$BH_2PH_2BH_2$·NMe_3]$^+$ (107.5(8)°) as a result of the steric influence of the attached IDipp moieties. The chain itself reveals a nearly antiperiplanar zigzag conformation with a torsion angle of −165.9(5)° (C1–B1–P1–Ga1).

Despite observing the formation of a stable, though highly air-sensitive chain compound, which decomposes slowly at room temperature, the question arose if the simultaneous stabilization by two bulky donors imposes a necessary requirement to keep the central structural motif intact or if the steric demand can be further reduced. Thus, PH_2BH_2·NMe_3 was reacted with **1a** by stirring in *o*-difluorobenzene at room temperature for 30 min (Eq. (2)). By subsequent layering with *n*-hexane at −30 °C, clear colourless plates of [IDipp · $GaH_2PH_2BH_2$·NMe_3][OTf] (**3b**) were obtained. **3b** shows a drastically higher sensitivity towards air than **3a** and decomposes faster at room temperature. Characteristic heteronuclear NMR data for **3b** are given in Table 1. Additionally, the ^{1}H NMR spectrum shows a broadened doublet at 3.60 ppm for the {GaH_2} unit ($^2J_{HP} = 33$ Hz) and a doublet of multiplets for the {PH_2} protons between 1.50 and 2.30 ppm ($^1J_{HP} = 322$ Hz). In the ESI-MS spectrum, the molecular ion peak of

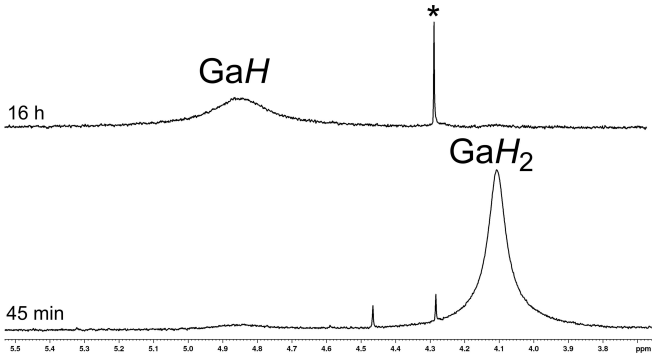

Figure 5. Comparison of sections of the ^{1}H NMR spectra of the reaction of exc. MeI with IDipp·GaH_3 after 45 min and after 16 h (C_6D_6, 298 K, * = unidentified impurity).

Table 1. Heteronuclear NMR chemical shifts ([ppm], 298 K) and signal multiplicities of compounds **3a**–**d**.[33]

NMR spectrum	**3a** CD_2Cl_2	**3b** CD_2Cl_2	**3c** CD_2Cl_2	**3d** o-DFB
^{31}P{^{1}H}	−168.2, s, br	−176.5, s, br	−39.9, s, br	−220.0, s
^{31}P	−168.2, t, br	−176.5, t, br	−39.9, s, br	−220.0, t(qt)
^{11}B{^{1}H}	−35.0, s, br	−11.3, s, br	−7.6, s, br	–
^{11}B	−35.0, s, br	−11.3, s, br	−7.6, s, br	–
^{19}F{^{1}H}	−79.1, s	−79.1, s	−78.7, s	−78.6, s

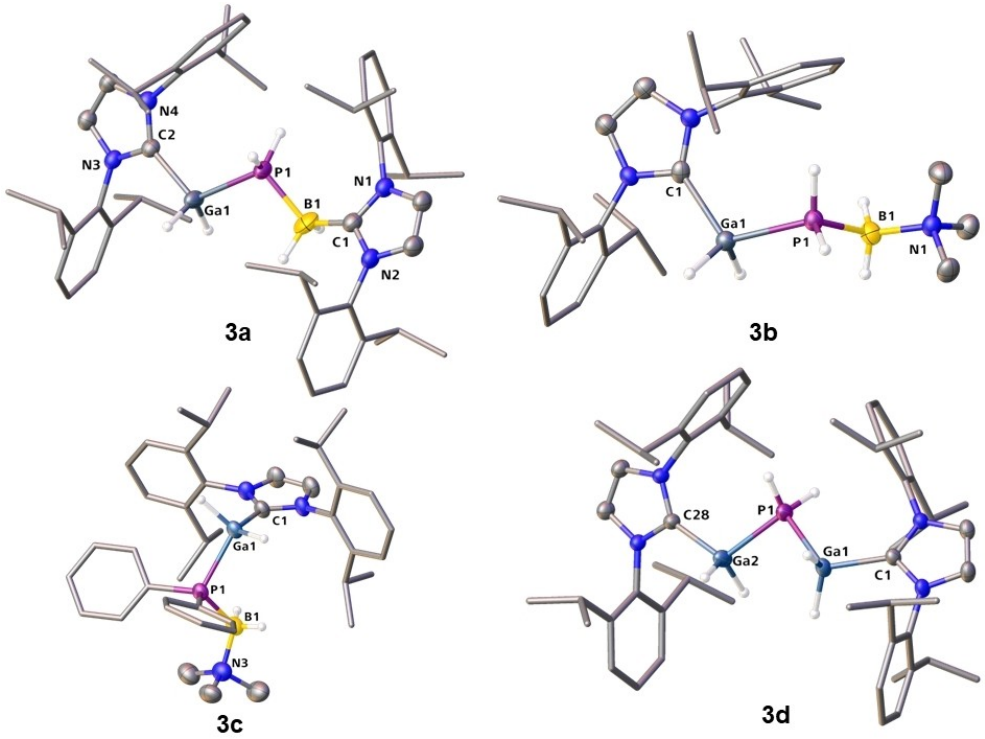

Figure 6. Molecular structures of **3a–d** in the solid state. Anisotropic displacement ellipsoids are shown at 50% probability level. Hydrogen atoms bound to carbon and the triflate anions are omitted for clarity. Dipp groups are displayed as a stick model for improved clarity. Selected bond lengths [Å] and angles [°]: **3a**: N1–C1 1.347(4), N2–C1 1.354(4), C1–B1 1.601(11), B1–P1 1.949(10), P1–Ga1 2.3731(15), Ga1–C2 2.055(3), C2–N3 1.355(3), C2–N4 1.343(3), N1–C1–B1 127.5(4), N2–C1–B1 127.2(4), C1–B1–P1 119.6(5), B1–P1–Ga1 103.8(3), P1–Ga1–C2 114.40(8), Ga1–C2–N3 120.92(19), Ga1–C2–N4 134.3(2). 3b: C1–Ga1 2.054(7), Ga1–P1 2.4002(16), P1–B1 1.959(8), B1–N1 1.597(9), C1–Ga1–P1 111.62(17), Ga1–P1–B1 111.5(2), P1–B1–N1 116.2(5). 3c: C1–Ga1 2.044(2), Ga1–P1 2.4007(7), P1–B1 1.965(3), B1–N3 1.612(4), C1–Ga1–P1 114.15(7), Ga1–P1–B1 106.99(9), P1–B1–N3 120.1(2). 3d: C1–Ga1 2.032(3), Ga1–P1 2.3831(10), P1–Ga2 2.3658(10), Ga2–C28 2.032(3), C1–Ga1–P1 112.85(10), Ga1–P1–Ga2 100.61(4), P1–Ga2–C28 113.95(10).

$[IDipp \cdot GaH_2PH_2BH_2 \cdot NMe_3]^+$ was detected at $m/z = 564.48$. **3b** crystallizes in the monoclinic space group *Cc* as clear colourless plates (Flack parameter: −0.01(3), Figure 6, top right)). The asymmetric unit contains one molecule of **3b** and does not show any disorder at the chain positions, in contrast to **3a** (cf. Supporting Information). The Ga–P distance is slightly elongated towards 2.400(15) Å compared to **3a** and is indicative of a weakened Ga–P bond. The B–P bond within **3b** is 1.960(8) Å long and has thus almost the same length as the B–P bond in **3a**. The Ga–P–B angle of 111.5(2) Å is significantly larger than that in **3a**, indicating the weaker steric influence of the NMe_3 group compared to IDipp in **3a**. Furthermore, the central chain is arranged in an antiperiplanar conformation with a Ga1–P1–B1–N1 torsion angle of −175.0(4)°.

Judging by the crystal structures of the parent compounds **3a** and **3b**, it could be assumed that the sterical arrangement should leave enough space to include organic residues at the chain motif. To test this hypothesis, **1a** was reacted with $NMe_3 \cdot BH_2PPh_2$ in *o*-difluorobenzene (Eq. (2)). By subsequent layering with *n*-hexane at −30 °C, large colourless crystals were obtained, which were identified as the desired chain compound $[IDipp \cdot GaH_2PPh_2BH_2 \cdot NMe_3][OTf]$ (**3c**) by multinuclear NMR spectroscopy, ESI-MS and X-ray crystallography (Figure 6, bottom left).

Just as **3a** and **3b**, **3c** displays high sensitivity towards air and decomposes at room temperature. **3c** shows characteristic, strongly broadened signals (see Table 1) in both ^{31}P and ^{11}B NMR spectra due to quadrupolar relaxation. The ^{1}H NMR spectrum features a broadened doublet at 3.92 ppm for the $\{GaH_2\}$ unit ($^2J_{HP} = 38$ Hz). In the ESI-MS spectrum, the molecular ion peak of $[IDipp \cdot GaH_2PPh_2BH_2 \cdot NMe_3]^+$ was detected at $m/z = 716.34$. **3c** crystallizes in the triclinic space group $P\bar{1}$ as clear colourless blocks (Figure 6). Overall, the bond lengths are very similar to those in **3b** (Ga–P: 2.4010(7) Å, P–B: 1.963(3) Å, B–N: 1.611(4) Å) and all within the range of single bonds. The same accounts for the corresponding bond angles (Ga–P–B: 107.03(9)°, P–B–N: 120.24(19)°). The chain motif is arranged in near perfect antiperiplanar conformation with a Ga1–P1–B1–N1 dihedral angle of 175.7(2)°.

Seeing how well the NHC-stabilized galliummonotriflates underwent nucleophilic substitution, it could be questioned whether NHC-stabilized phosphanylgallane $IDipp \cdot GaH_2PH_2$ as an even weaker donor would also undergo such a transformation. Although such a symmetric species would impose a certain stability, the low Ga–P bonding energy might prevent the isolation of the desired cationic chain compound. Thus, a mixture of **1a** and $IDipp \cdot GaH_2PH_2$ in *o*-difluorobenzene was stirred for 30 min and the reaction mixture layered with *n*-hexane at −30 °C (Eq. (2)). That way, highly air-sensitive crystals

of [IDipp·GaH$_2$PH$_2$GaH$_2$·IDipp][OTf] (**3 d**) were obtained after two weeks, which decompose at room temperature (Figure 6). **3 d** represents the first example of the parent 2e-donor-stabilized 13/15 cationic chain compound including only heavy group 13 elements. **3 d** displays extreme lability and immediately converts back to the starting materials when dissolved in THF or CH_2Cl_2. However, **3 d** is stable in *o*-difluorobenzene, indicating that the IDipp·GaH$_2$PH$_2$ unit is easily replaced by other donor molecules. The ^{31}P NMR spectrum of **3 d** in a solution of 1,2-difluorobenzene (C_6D_6-capillary, r.t.) shows a triplet of quintets at −220.0 ppm with coupling constants of $^1J_{HP}$ = 278 Hz and $^2J_{HP}$ = 45 Hz. In the ESI-MS spectrum, strong fragmentation together with the release of methane is observed, leading to a molecular ion peak of {[IDipp·GaH$_2$PH$_2$GaH$_2$·IDipp]$^+$–CH$_4$} diminished by methane at *m/z* = 937.50. **3 d** crystallizes as clear irregular blocks in the acentric orthorhombic space group *Pna*2$_1$ (Figure 6, bottom right; Flack parameter −0.044(15)). The structure in the solid state adapts a slightly distorted arrangement with a highly bent central Ga1–P–Ga2 bond angle of 100.61(4)°. The Ga–P bond lengths of 2.3658(9) Å and 2.3831(10) Å are slightly asymmetric due to steric reasons and within the range of single bonds. The C1–Ga1–P1–Ga1 torsion angle of 147.76(11)° reveals an anticlinal conformation.

To further examine the bonding situation of the obtained chain compounds, quantum chemical computations were performed (Table 2). According to NPA charge analysis[30] (TPSSh/def2-TZVP//B3LYP-D4/def2-TZVP),[27,28,31] the central chain motifs display a large degree of polarization. Compound **3 a**, for example, bears a total charge of +0.43 for the entire {GaH$_2$PH$_2$BH$_2$} core structure and thus highlights the electron deficiency compensated by the two donors. **3 c**–**d** show a similar trend (Table 2), though the phenyl rings at **3 c** overall reduce the positive charge on the chain structure.

Furthermore, the H atoms at Ga also display a considerably hydridic character in contrast to the H atoms at B. The Wiberg Bond Indices (WBI) for all P–B and P–Ga bonds describe single bonds between the atom pairs, although the WBIs remain significantly lower for the P–Ga bonding due to the weak bond strengths, which also explains the thermal instability of **3 a**–**d**. The NBO analysis also shows, that the core motifs are made up by regular **2 c**–**2 e** σ-bonds between the pnictogen and the triel atoms with the main contribution coming from the pnictogen (see Supporting Information).

Table 2. Calculated Natural Charges *q*, Wiberg Bond Indices (WBI) and sum of charges of the central {GaH$_2$PR$_2$EH$_2$} chain motif *Q*(chain) for compounds **3 a**–**d** as calculated by NBO computations.

Calc. Property	3 a	3 b	3 c	3 d
q(Ga)	+0.64	+0.67	+0.65	+0.64
q(P)	+0.22	+0.17	+0.73	−0.18
q(B)	−0.51	−0.24	−0.23	–
q(H$_P$)	+0.24	+0.29	–	+0.46
q(H$_{Ga}$)	−0.24	−0.23	−0.24	−0.24
q(H$_B$)	+0.04	+0.01	−0.01	–
Q(Chain)	+0.43	+0.74	+0.23	+1.06
WBI (Ga–P)	0.67	0.64	0.62	0.69
WBI (P–B)	0.96	1.00	0.97	–

Conclusions

In summary, the novel NHC- stabilized galliummonotriflates IDipp·GaH$_2$(OTf) (**1 a**), IPr$_2$Me$_2$·GaH$_2$(OTf) (**1 b**), and IMes·GaH$_2$(OTf) (**1 c**) were synthesized in high yields. **1 c** adapts a one-dimensional polymeric structure in the solid state compared to **1 a**, which does not show an oligomerized structure. Our experimental investigations demonstrate that the degree of substitution of such triflation or iodination reactions can be easily controlled via the reaction time. This is further supported by quantum chemical computations, which indicate that the second reaction step proceeds much slower due to a higher activation barrier. By reacting different donor-stabilized pnictogenylboranes with IDipp·GaH$_2$(OTf) (**1 a**), the unprecedented, extremely air-sensitive parent Ga/15/13 chain compounds [IDipp·GaH$_2$PH$_2$BH$_2$·IDipp][OTf] (**3 a**), [IDipp·GaH$_2$PH$_2$BH$_2$·NMe$_3$][OTf] (**3 b**) and [IDipp·GaH$_2$PPh$_2$BH$_2$·NMe$_3$][OTf] (**3 c**) were synthesized and comprehensively characterized. All obtained products show pronounced instability at room temperature. By reacting **1 a** with IDipp·GaH$_2$PH$_2$, it was also possible to synthesize the first cationic 13/15 three-membered parent chain compound that only contains heavy group 13 homologues, [IDipp·GaH$_2$PH$_2$GaH$_2$·IDipp][OTf] (**3 d**), which, besides the aforementioned sensitivity towards air and temperature, is also only stable in *o*-difluorobenzene. Quantum chemical calculations highlight the strongly polarized bonding situation along the central chain motifs.

Experimental Section

Experimental procedures, full analytical data and details regarding quantum chemical calculations are described in the Supporting Information.

Deposition Number(s) 2263441 (**1 a**), 2263442 (**1 b**), 2263443 (**3 a**), 2263444 (**3 b**), 2263445 (**3 c**) and, 2263446 (**3 d**) contain(s) the supplementary crystallographic data for this paper. These data are provided free of charge by the joint Cambridge Crystallographic Data Centre and Fachinformationszentrum Karlsruhe Access Structures service.

Acknowledgements

This work was supported by the Deutsche Forschungsgemeinschaft (DFG) within the project Sche 384/41-1. R.S. is grateful to the Fonds der Chemischen Industrie (FCI) for a PhD fellowship. Lisa Zimmermann, Christoph Riesinger, Matthias T. Ackermann, Felix Lehnfeld and Dr. Michael A. K. Weinhart are thanked for fruitful discussions and providing several starting materials. Felix Lehnfeld and Lukas Adlbert are acknowledged for their

assistance with ESI-MS measurements. Open Access funding enabled and organized by Projekt DEAL.

Conflict of Interests

The authors declare no conflict of interest.

Data Availability Statement

The data that support the findings of this study are available in the supplementary material of this article.

Keywords: cationic chain compounds · 13/15 compounds · pentelyltrielanes · pnictogen · triels

[1] a) C. E. Housecroft, A. Sharpe, *Inorganic Chemistry*, 4. Aufl., Pearson, New York, **2012**, 859–861; b) A. C. Jones, P. O'Brien, *CVD of Compound Semiconductors: Precursor Synthesis Development and Applications*, VCH, Weinheim, **1996**; c) M. R. Leys, *Chemtronics* **1987**, *2*, 155–164; d) G. B. Stringfellow, *Rep. Prog. Phys.* **1982**, *45*, 469–525; e) R. A. Fischer, J. Weiß, *Angew. Chem. Int. Ed.* **1999**, *38*, 2830–2850; *Angew. Chem.* **1999**, *111*, 3002–3022; f) J. D. Masuda, A. J. Hoskin, T. W. Graham, C. Beddie, M. C. Fermin, N. Etkin, D. W. Stephan, *Chem. Eur. J.* **2006**, *12*, 8696–8707; g) R. D. Wells, W. L. Gladfelter, *J. Cluster Sci.* **1997**, *8*, 217–238.

[2] a) A. B. Burg, H. I. Schlesinger, *J. Am. Chem. Soc.* **1937**, *59*, 780–787; b) J. Gay-Lussac, J. Thenard, *Mem. Phys. Chim. Soc. d'Arcueil* **1809**, *2*, 210–211; c) A. Stock, E. Pohland, *Chem. Ber.* **1926**, *59*, 2210–2215.

[3] a) A. H. Cowley, R. A. Jones, *Angew. Chem. Int. Ed.* **1989**, *28*, 1208–1215; *Angew. Chem.* **1989**, *101*, 1235–1243; b) J. F. Janik, R. L. Wells, V. G. Young, A. L. Rheingold, I. A. Guzei, *J. Am. Chem. Soc.* **1998**, *120*, 532–537; c) S. M. Stuczynski, R. L. Opila, P. Marsh, J. G. Brennan, M. L. Steigerwald, *Chem. Mater.* **1991**, *3*, 379–381.

[4] a) C. W. Hamilton, R. T. Baker, A. Staubitz, I. Manners, *Chem. Soc. Rev.* **2009**, *38*, 279–293; b) R. Hoffmann, *J. Chem. Phys.* **1964**, *40*, 2474–2480; c) A. Staubitz, A. P. M. Robertson, M. E. Sloan, I. Manners, *Chem. Rev.* **2010**, *110*, 4023–4078.

[5] a) J.-M. Denis, H. Forintos, H. Szelke, L. Toupet, T.-N. Pham, P.-J. Madec, A.-C. Gaumont, *Chem. Commun.* **2003**, 54–55; b) P. P. Power, *Chem. Rev.* **1999**, *99*, 3463–3503.

[6] a) M. Kapitein, M. Balmer, L. Niemeier, C. von Hänisch, *Dalton Trans.* **2016**, *45*, 6275–6281; b) M. Kapitein, M. Balmer, C. von Hänisch, *Z. Anorg. Allg. Chem.* **2016**, *642*, 1275–1281; c) O. Lemp, M. Balmer, K. Reiter, F. Weigend, C. von Hänisch, *Chem. Commun.* **2017**, *53*, 7620–7623; d) D. W. N. Wilson, W. K. Myers, J. M. Goicoechea, *Dalton Trans.* **2020**, *49*, 15249–15255; e) A. K. Swarnakar, C. Hering-Junghans, K. Nagata, M. J. Ferguson, R. McDonald, N. Tokitoh, E. Rivard, *Angew. Chem. Int. Ed.* **2015**, *54*, 10666–10669; f) A. Heilmann, J. Hicks, P. Vasko, J. M. Goicoechea, S. Aldridge, *Angew. Chem. Int. Ed.* **2020**, *132*, 4927–4931; g) J. Hicks, P. Vasko, J. M. Goicoechea, S. Aldridge, *Nature* **2018**, *557*, 92–95; h) D. W. N. Wilson, J. Feld, J. M. Goicoechea, *Angew. Chem. Int. Ed.* **2020**, *132*, 21100–21104; i) A. Bücker, C. Wölper, G. Haberhauer, S. Schulz, *Chem. Commun.* **2022**, *58*, 9758–9761; j) C. Ganesamoorthy, C. Helling, C. Wölper, W. Frank, E. Bill, G. E. Cutsail, S. Schulz, *Nat. Commun.* **2018**, *9*, 87; k) S. Ghosh, E. Glöckler, C. Wölper, J. Linders, N. Janoszka, A. H. Gröschel, S. Schulz, *Eur. J. Inorg. Chem.* **2022**, *2022*; l) C. Helling, C. Ganesamoorthy, C. Wölper, S. Schulz, *Dalton Trans.* **2022**, *51*, 2050–2058; m) C. Helling, C. Wölper, S. Schulz, *J. Am. Chem. Soc.* **2018**, *140*, 5053–5056; n) C. Helling, C. Wölper, Y. Schulte, G. E. Cutsail III, S. Schulz, *Inorg. Chem.* **2019**, *58*, 10323–10332; o) C. Helling, C. Wölper, S. Schulz, *Eur. J. Inorg. Chem.* **2020**, *2020*, 4225–4235; p) C. Helling, C. Wölper, S. Schulz, *Dalton Trans.* **2020**, *49*, 11835–11842; q) J. Krüger, C. Ganesamoorthy, L. John, C. Wölper, S. Schulz, *Chem. Eur. J.* **2018**, *24*, 9157–9164; r) J. Krüger, C. Wölper, G. Haberhauer, S. Schulz, *Inorg. Chem.* **2022**, *61*, 597–604; s) J. Krüger, C. Wölper, S. Schulz, *Angew. Chem. Int. Ed.* **2021**, *60*, 3572–3575; t) B. Li, C. Wölper, G. Haberhauer, S. Schulz, *Angew. Chem. Int. Ed.* **2021**, *133*, 2014–2019; u) B. Li, B. L. Geoghegan, H. M. Weinert, C. Wölper, G. E. Cutsail, S. Schulz, *Chem. Commun.* **2022**, *58*, 4372–4375; v) J. Schoening, L. John, C. Wölper, S. Schulz, *Dalton Trans.* **2019**, *48*, 17729–17734; w) M. K. Sharma, C. Wölper, G. Haberhauer, S. Schulz, *Angew. Chem. Int. Ed.* **2021**, *60*, 6784–6790; x) M. K. Sharma, P. Dhawan, C. Helling, C. Wölper, S. Schulz, *Chem. Eur. J.* **2022**, *28*, e202200444; y) M. K. Sharma, C. Wölper, S. Schulz, *Dalton Trans.* **2022**, *51*, 1612–1616; z) H. M. Weinert, C. Wölper, S. Schulz, *Chem. Sci.* **2022**, *13*, 3775–3786; S. Schneider, C. Hänisch, *Eur. J. Inorg. Chem.* **2021**, *2021*, 4655–4660.

[7] a) A. Adolf, M. Zabel, M. Scheer, *Eur. J. Inorg. Chem.* **2007**, *2007*, 2136–2143; b) C. A. Jaska, A. J. Lough, I. Manners, *Inorg. Chem.* **2004**, *43*, 1090–1099; c) U. Vogel, P. Hoemensch, K.-C. Schwan, A. Y. Timoshkin, M. Scheer, *Chem. Eur. J.* **2003**, *9*, 515–519; d) U. Vogel, A. Y. Timoshkin, M. Scheer, *Angew. Chem. Int. Ed.* **2001**, *40*, 4409–4412.

[8] a) J. A. Bailey, M. F. Haddow, P. G. Pringle, *Chem. Commun.* **2014**, *50*, 1432–1434; b) J. A. Bailey, M. Ploeger, P. G. Pringle, *Inorg. Chem.* **2014**, *53*, 7763–7769; c) J. A. Bailey, P. G. Pringle, *Coord. Chem. Rev.* **2015**, *297*, 77–90; d) J. M. Breunig, A. Hübner, M. Bolte, M. Wagner, H.-W. Lerner, *Organometallics* **2013**, *32*, 6792–6799; e) T. Chen, E. N. Duesler, H. Nöth, R. T. Paine, *J. Organomet. Chem.* **2000**, *614–615*, 99–106; f) T. Chen, J. Jackson, S. A. Jasper, E. N. Duesler, H. Nöth, R. T. Paine, *J. Organomet. Chem.* **1999**, *582*, 25–31; g) F. Dankert, C. Hering-Junghans, *Chem. Commun.* **2022**, *58*, 1242–1262; h) D. Dou, G. W. Linti, T. Chen, E. N. Duesler, R. T. Paine, H. Nöth, *Inorg. Chem.* **1996**, *35*, 3626–3634; i) S. J. Geier, T. M. Gilbert, D. W. Stephan, *Inorg. Chem.* **2011**, *50*, 336–344; j) S. J. Geier, T. M. Gilbert, D. W. Stephan, *J. Am. Chem. Soc.* **2008**, *130*, 12632–12633; k) M. Kaaz, J. Bender, D. Förster, W. Frey, M. Nieger, D. Gudat, *Dalton Trans.* **2014**, *43*, 680–689; l) M. A. Mardones, A. H. Cowley, L. Contreras, R. A. Jones, *J. Organomet. Chem.* **1993**, *455*, C1–C2; m) K. M. Simpson, R. W. Gedridge JR, K. T. Higa, *J. Organomet. Chem.* **1993**, *456*, 31–34; n) A. M. Spokoyny, C. D. Lewis, G. Teverovskiy, S. L. Buchwald, *Organometallics* **2012**, *31*, 8478–8481; o) A. Tsurusaki, T. Sasamori, A. Wakamiya, S. Yamaguchi, K. Nagura, S. Irle, N. Tokitoh, *Angew. Chem. Int. Ed.* **2011**, *123*, 11132–11135; p) N. E. Stubbs, T. Jurca, E. M. Leitao, C. H. Woodall, I. Manners, *Chem. Commun.* **2013**, *49*, 9098–9100.

[9] O. Hegen, A. V. Virovets, A. Y. Timoshkin, M. Scheer, *Eur. J. Inorg. Chem.* **2018**, *24*, 16521–16525.

[10] F. Lehnfeld, M. Seidl, A. Y. Timoshkin, M. Scheer, *Eur. J. Inorg. Chem.* **2022**, *3*, e202100930.

[11] a) C. Marquardt, A. Adolf, A. Stauber, M. Bodensteiner, A. V. Virovets, A. Y. Timoshkin, M. Scheer, *Chem. Eur. J.* **2013**, *19*, 11887–11891; b) C. Marquardt, T. Kahoun, J. Baumann, A. Y. Timoshkin, M. Scheer, *Z. Anorg. Allg. Chem.* **2017**, *643*, 1326–1330; c) K.-C. Schwan, A. Y. Timoskin, M. Zabel, M. Scheer, *Chem. Eur. J.* **2006**, *12*, 4900–4908.

[12] a) M. Elsayed Moussa, T. Kahoun, M. T. Ackermann, M. Seidl, M. Bodensteiner, A. Y. Timoshkin, M. Scheer, *Organometallics* **2022**, *41*, 1572–1578; b) C. Marquardt, T. Kahoun, A. Stauber, G. Balázs, M. Bodensteiner, A. Y. Timoshkin, M. Scheer, *Angew. Chem. Int. Ed.* **2016**, *55*, 14828–14832.

[13] M. T. Ackermann, M. Seidl, F. Wen, M. J. Ferguson, A. Y. Timoshkin, E. Rivard, M. Scheer, *Chem. Eur. J.* **2022**, *28*, e20210370.

[14] C. Marquardt, G. Balázs, J. Baumann, A. V. Virovets, M. Scheer, *Chem. Eur. J.* **2017**, *23*, 11423–11429.

[15] C. Marquardt, C. Thoms, A. Stauber, G. Balázs, M. Bodensteiner, M. Scheer, *Angew. Chem. Int. Ed.* **2014**, *53*, 3727–3730.

[16] a) M. Bodensteiner, A. Y. Timoshkin, E. V. Peresypkina, U. Vogel, M. Scheer, *Chem. Eur. J.* **2013**, *19*, 957–963; b) M. Bodensteiner, U. Vogel, A. Y. Timoshkin, M. Scheer, *Angew. Chem. Int. Ed.* **2009**, *48*, 4629–4633; c) C. Marquardt, T. Jurca, K.-C. Schwan, A. Stauber, A. V. Virovets, G. R. Whittell, I. Manners, M. Scheer, *Angew. Chem. Int. Ed.* **2015**, *54*, 13782–13786; d) C. Thoms, C. Marquardt, A. Y. Timoshkin, M. Bodensteiner, M. Scheer, *Angew. Chem. Int. Ed.* **2013**, *52*, 5150–5154; e) C. Marquardt, O. Hegen, A. Vogel, A. Stauber, M. Bodensteiner, A. Y. Timoshkin, M. Scheer, *Chem. Eur. J.* **2018**, *24*, 360–363.

[17] a) J. Braese, A. Schinabeck, M. Bodensteiner, H. Yersin, A. Y. Timoshkin, M. Scheer, *Chem. Eur. J.* **2018**; b) M. Elsayed Moussa, J. Braese, C. Marquardt, M. Seidl, M. Scheer, *Eur. J. Inorg. Chem.* **2020**, *26*, 2501–2505; c) M. Elsayed Moussa, C. Marquardt, O. Hegen, M. Seidl, M. Scheer, *New J. Chem.* **2021**, *45*, 14916–14919; d) K.-C. Schwan, A. Adolf, M. Bodensteiner, M. Zabel, M. Scheer, *Z. Anorg. Allg. Chem.* **2008**, *634*, 1383–1387.

[18] C. Marquardt, O. Hegen, T. Kahoun, M. Scheer, *Chem. Eur. J.* **2017**, *23*, 4397–4404.

[19] M. A. K. Weinhart, A. S. Lisovenko, A. Y. Timoshkin, M. Scheer, *Angew. Chem. Int. Ed.* **2020**, *59*, 5541–5545; *Angew. Chem.* **2020**, *132*, 5586–5590.

[20] M. A. K. Weinhart, M. Seidl, A. Y. Timoshkin, M. Scheer, *Angew. Chem.* **2021**, *133*, 3850–3855; *Angew. Chem. Int. Ed.* **2021**, *60*, 3806–3811.
[21] A. Y. Timoshkin, G. Frenking, *Inorg. Chem.* **2003**, *42*, 60–69.
[22] M. Gonsior, I. Krossing, *Z. Anorg. Allg. Chem.* **2002**, *628*, 1821–1830.
[23] A. Hock, L. Werner, M. Riethmann, U. Radius, *Eur. J. Inorg. Chem.* **2020**, *42*, 4015–4023.
[24] P. Pyykkö, M. Atsumi, *Chem. Eur. J.* **2009**, *15*, 12770–12779.
[25] A. K. Swarnakar, M. J. Ferguson, R. McDonald, E. Rivard, *Dalton Trans.* **2017**, *46*, 1406–1412.
[26] a) A. D. Becke, *J. Chem. Phys.* **1993**, *98*, 5648–5652; b) C. Lee, W. Yang, R. G. Parr, *Phys. Rev. B* **1988**, *37*, 785–789; c) Y. Guo, C. Riplinger, U. Becker, D. G. Liakos, Y. Minenkov, L. Cavallo, F. Neese, *J. Chem. Phys.* **2018**, *148*, 11101; d) V. Ásgeirsson, B. O. Birgisson, R. Bjornsson, U. Becker, F. Neese, C. Riplinger, H. Jónsson, *J. Chem. Theory Comput.* **2021**, *17*, 4929–4945; e) F. Weigend, R. Ahlrichs, *Phys. Chem. Chem. Phys.* **2005**, *7*, 3297–305; f) F. Neese, *WIREs Comput. Mol. Sci.* **2012**, *2*, 73–78; g) F. Neese, *WIREs Comput. Mol. Sci.* **2018**, *8*, e1327; h) F. Neese, *WIREs Comput. Mol. Sci.* **2022**, *12*, e1606; i) F. Neese, F. Wennmohs, U. Becker, C. Riplinger, *J. Chem. Phys.* **2020**, *152*, 224108.
[27] E. Caldeweyher, C. Bannwarth, S. Grimme, *J. Chem. Phys.* **2017**, *147*, 34112.
[28] E. Caldeweyher, S. Ehlert, A. Hansen, H. Neugebauer, S. Spicher, C. Bannwarth, S. Grimme, *J. Chem. Phys.* **2019**, *150*, 154122.
[29] a) M. G. Evans, M. Polanyi, *Trans. Faraday Soc.* **1935**, *31*, 875–894; b) H. Eyring, *J. Chem. Phys.* **1935**, *3*, 107–115.
[30] A. E. Reed, L. A. Curtiss, F. Weinhold, *Chem. Rev.* **1988**, *88*, 899–926.
[31] a) A. D. Becke, *Phys. Rev. A* **1988**, *38*, 3098–3100; b) J. P. Perdew, *Phys. Rev. B* **1986**, *33*, 8822–8824; c) V. N. Staroverov, G. E. Scuseria, J. Tao, J. P. Perdew, *J. Chem. Phys.* **2003**, *119*, 12129–12137.
[32] Given yields refer to the isolated amounts of product at room temperature.
[33] NMR samples were prepared quickly at room temperature and measured directly after sample preparation.

Manuscript received: June 1, 2023
Accepted manuscript online: July 4, 2023
Version of record online: ■■, ■■

RESEARCH ARTICLE

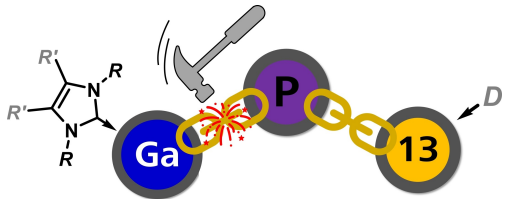

A general synthetic pathway towards NHC-stabilized galliumtriflates $NHC \cdot GaH_2(OTf)$ (NHC = IDipp, IMes, IPr_2Me_2) is reported. These compounds were used as building blocks to obtain unprecedented 13/15 cationic chain compounds of the heavier group 13 elements $[IDipp \cdot GaH_2PR_2EH_2 \cdot D]$ (R = H, Ph; D = NMe_3, IDipp; E = B, Ga). All compounds were characterized by single-crystal X-ray structure determination and the electronic features were elucidated by computational methods.

*R. Szlosek, Dr. M. Seidl, Dr. G. Balázs, Prof. Dr. M. Scheer**